2018 IEEE 20th International Conference on High Performance Computing and Communications; IEEE 16th International Conference on Smart City; IEEE 4th Intl. Conference on Data Science and Systems

SAW Delay Line based IoT Smart Sensing in Water Distribution System

Zhaozhao Tang
School of Computing and Digital Technologies
Staffordshire University
Stoke on Trent, ST4 2DE, United Kingdom
zhaozhao.tang@research.staffs.ac.uk

Wenyan Wu
School of Engineering and the Built Environment
Birmingham City University
Birmingham, B4 7XG, United Kingdom
wenyan.wu@bcu.ac.uk

Jinliang Gao
School of Municipal and Environmental Engineering
Harbin Institute of Technology
Harbin, 150090, P. R. China
gjl@hit.edu.cn

Po Yang
Faculty of Engineering and Technology
Liverpool John Moores University
Liverpool, L3 3AF, United Kingdom
p.yang@ljmu.ac.uk

***Abstract*—Wireless Passive Surface Acoustic Wave (SAW) sensors have attracted great attention in numerous applications. They are powered by interrogating Radio Frequency (RF) pulses rather than batteries. In this study, a wireless passive SAW temperature and pressure delay line sensor was adapted in a designed framework which can control the ambient liquid temperature and pressure and characterised. The experimental results meet the theoretical analysis that the related phase delay of the response signal depends linearly on the temperature (pressure) when the pressure (temperature) keeps constant.**

Keywords—SAW; sensor; phase; temperature; pressure

I. INTRODUCTION

Wireless passive SAW sensors provide the capability of sensing physical quantities, e.g., temperature [1, 2], pressure [3], torsion [4], flow rate [5] etc. without direct power supply (batteries are not necessary power sources for sensor nodes). They are powered and activated by absorbing the energy of the interrogation RF pulses. There are many advantages of using the wireless passive SAW sensors apart from their wireless access and passive elements characters, e.g. small size, high sensitivity, ruggedized elements and suitable to use in harsh environment [6].

Internet of Things (IoT) technology has been widely applied to a variety of industrial projects, e.g. healthcare, manufacture, energy consumption, etc. [8-13]. Smart sensors can be a form of IoT, a network of technologies which can monitor both physical and chemical parameters, capture meaningful data, and communicate that data over a wireless network to a computer in the cloud for software to analyse in real time and help determine action steps. Technologies are capable of monitoring objects such as smart water meters and other electronic devices, organisms, or a natural part of the environment such as an area of ground to be measured for moisture or chemical content. A smart device is associated with each object which provides the connectivity and a unique digital identity for identifying, tracking, and communicating with the object [14, 15]. A sensor within or attached to the device is connected to the internet by a local area connection (such as RFID, NFC, or BTLE) and can also have wide area connectivity. Typically, each data transmission from a device is small, but the number of transmissions can be frequent. IoT involves many, many things interacting with each other to produce actionable information [8-10, 12, 13].

The present work aims to characterise the wireless passive temperature and pressure SAW sensor and evaluate the performance of it for liquid temperature and pressure sensing. The sensor node was adapted into a designed two-layer glass pipe experimental framework to simulate the ambient liquid environment. The adapted SAW sensor node was interrogated by using a vector signal generator, and a signal analyser and an oscilloscope were used for receiving the response signals and the subsequent processing steps. Temperature changes were applied by the water bath, and pressure changes were controlled by the liquid pressure transmission platform.

II. SENSOR NODE STRUCTURE

The fundamental structure of the wireless passive SAW temperature and pressure sensor is shown in Fig. 1, which consists of a SAW delay line with an antenna connected with the Inter Digital Transducers (IDT). The SAW sensor obtains the necessary energy from the RF signal received through the antenna. In this case, the SAW sensor contains a minimum number of elements and there are no power supply components, such as batteries, in this design. The outside pressure applied through the action point is different from the reference pressure inside the sensor. The pressure differences act on the left part of the substrate, and the temperature affects the whole substrate at the same time by the bonding basis on the right of the substrate. The RF signal can be received and sent through the connected antenna and converted by the IDT. Reflectors are manufactured in parallel with the IDT on the substrate to reflect the SAW. Two

978-1-5386-6614-2/18/$31.00 ©2018 IEEE
DOI 10.1109/HPCC/SmartCity/DSS.2018.00243

are located at the right side of the IDT (R_2 and R_3) and one is on the left (R_1). Such a design can fully use the two opposite directions SAW energy propagating from the IDT [7].

The dimensions of the top surface of the substrate change with the change of temperature and pressure. Consequently, the time delays caused by the SAW propagations are different, which leads to the phase shifts. In the case of this SAW sensor, the interrogator transmits a pulse signal, and the sensor responds with a chain of pulses depending on the positions of the reflectors arranged on the substrate's surface. The different time delays between two or more response signals are evaluated. The current pressure and temperature information is acquired from the response signals through the subsequent signal processing.

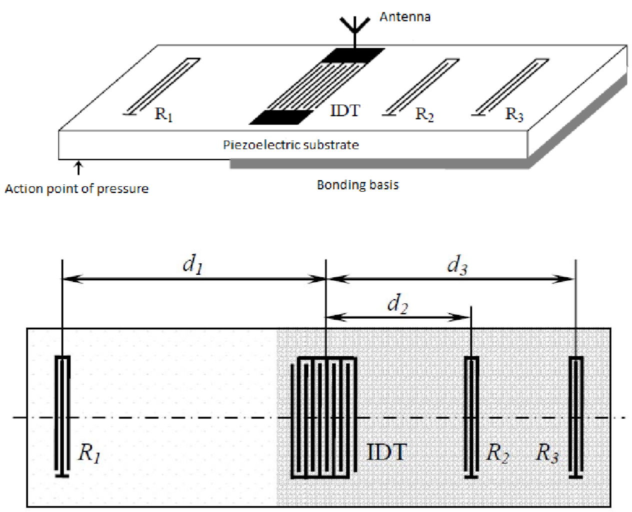

Fig. 1. The structure of the wireless passive delay line SAW temperature and pressure sensor node.

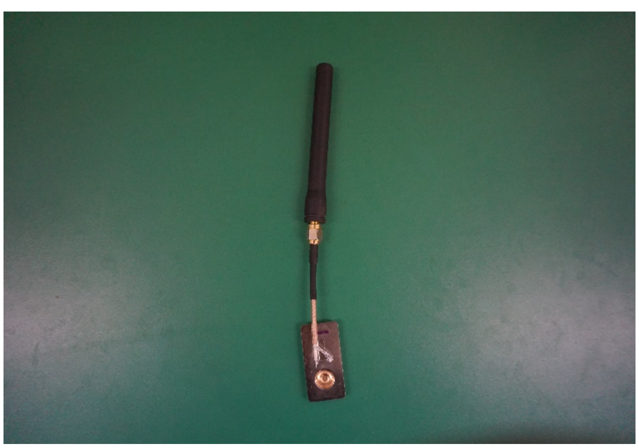

Fig. 2. The photo of wireless passive SAW delay line temperature and pressure sensor node with antenna.

Fig. 2 shows the sensor node of the wireless passive SAW delay line temperature and pressure sensor node with the antenna. To achieve better experiment performance, the performance of various antennas was investigated, the connected antenna was changed from the spiral type in the previous study [3, 16] to this current type for enhance the signal strength.

III. THEORETICAL MODEL

Based on the theory of SAW and the sensor structure, the values of temperature and pressure can be determined by the following equations. The initial RF interrogation signal transmitted from the reader antenna $S(t)$ is given by Equation 1.

$$S(t) = A\cos(\omega_0 t + \theta_0) = A\cos[\theta(t)] \qquad (1)$$

where ω_0 is the initial angular velocity; t is the time; θ_0 is the initial phase of the interrogation signal; A is the initial amplitude of the interrogation signal.

The RF response signal reflected by R_i (i=1, 2, 3) reflector is given by Equation 2.

$$S_i(t) = A_i\cos[\omega_0(t - t_i) + \theta_0] = A_i\cos[\theta_i(t)] \qquad (2)$$

where t_i is time delay of the RF response signal reflected by R_i (i=1, 2, 3) reflector against the interrogation signal; A_i is the amplitude of the response signal reflected by R_i (i=1, 2, 3) reflector, which is normally a smaller value than A due to attenuation of propagation.

The time delay t_i consists of two parts shown by Equation 3, one is τ_i, the time delay caused by the SAW propagation from the IDT to the R_i (i=1, 2, 3) reflector and the back way to the IDT, and the other one is τ_e, the delay caused by other reasons, e.g. the time delay caused by the RF signal propagates between the antenna of the reader and the antenna of the SAW sensor. τ_e is a constant value for all the response signals. τ_i can be derived by d_i, the distance from the IDT to the R_i (i=1, 2, 3) reflector and v, the velocity of the SAW propagation on the substrate.

$$t_i = \tau_i + \tau_e = \frac{2d_i}{v} + \tau_e \qquad (3)$$

From the sensor structure, reflector R_2 and R_3 are used for temperature measurement. φ_T is defined as the phase difference directly indicating the temperature impact of the ambient environment, which is derived in Equation 4. τ_e is taken out by the subtraction.

$$\varphi_T = \varphi_3 - \varphi_2 = \omega_0(t_3 - t_2) = \omega_0(\tau_3 - \tau_2) = \omega_0\tau_T \qquad (4)$$

where τ_T is the time delay of the SAW propagation from R_2 to R_3 and reflected back from R_3 to R_2.

The relation of τ_T and the temperature T to be sensed is shown is Equation 5.

$$\tau_T = \frac{2(d_3 - d_2)}{v} = \frac{2d_T}{v} = \tau_{T_0}[1 + \alpha(T - T_0)] \qquad (5)$$

where d_T is the distance between R_2 and R_3 on the surface of the sensor substrate; τ_{T_0} is the time delay caused by the SAW propagation from R_2 to R_3 reflector and the back way to R_2 at the initial temperature T_0; α is the temperature coefficient of the sensor substrate material.

τ_{T_0} can be derived by Equation 6, in which d_{T_0} is the distance between R_2 and R_3 on the surface of the sensor substrate at the initial temperature T_0.

$$\tau_{T_0} = \frac{2d_{T_0}}{v} \qquad (6)$$

According to the propagation theory of SAW, the initial angular velocity ω_0 is derived in Equation 7, where f_0 the initial frequency corresponding to ω_0.

$$\omega_0 = 2\pi f_0 \qquad (7)$$

Equation 8 shows the relation between the velocity of the SAW propagation on the substrate v and f_0, in which λ is the wavelength of the SAW propagating on the surface of the sensor substrate.

$$v = f_0 \lambda \qquad (8)$$

φ_{T_0} is defined as the phase difference directly indicating the temperature impact of the ambient environment at the initial temperature T_0. Equation 9 shows the relation between φ_{T_0} and τ_{T_0} in a similar way as Equation 4.

$$\varphi_{T_0} = \omega_0 \tau_{T_0} \qquad (9)$$

Summarising Equation 4 – 9, the temperature change ΔT can be derived using the change of the phase difference directly indicating the temperature impact of the ambient environment $\Delta\varphi_T$.

$$\Delta T = T - T_0 = \frac{\lambda}{4\pi\alpha d_{T_0}}\left(\varphi_T - \varphi_{T_0}\right) = \frac{\lambda}{4\pi\alpha d_{T_0}}\Delta\varphi_T \qquad (10)$$

Equation 10 shows the linear relation between ΔT and $\Delta\varphi_T$, which can be used to characterise the SAW sensor device.

From the sensor structure, the time delay t_1 is influenced by both temperature and pressure change. In order to separate the independent impact information caused by pressure change from the response signal reflected by R_1, compensation method should be used to eliminate the impact caused by temperature change.

Like Equation 4, the phase difference between the response signals reflected by R_1 and R_2 φ_{PT} is derived in Equation 11.

$$\varphi_{PT} = \varphi_1 - \varphi_2 = \omega_0(t_1 - t_2) = \omega_0(\tau_1 - \tau_2) = \omega_0 \tau_{PT} \qquad (11)$$

where τ_{PT} is the SAW propagation time difference between SAW propagating from the IDT to R_1 and reflected back to the IDT and it propagating from the IDT to R_2 and reflected back to the IDT.

μ_T is defined as the average strain caused by temperature change, and μ_P is defined as the average strain caused by pressure change (see Equation 12 and 13).

$$\mu_T = \alpha(T - T_0) = \alpha\Delta T \qquad (12)$$

$$\mu_P = \beta(P - P_0) = \beta\Delta P \qquad (13)$$

where β is the pressure coefficient of the sensor substrate material; P is the pressure to be sensed; P_0 is the initial pressure; ΔP is the pressure change.
τ_{PT} can be derived by Equation 14.

$$\tau_{PT} = \frac{2(d_1 - d_2)}{v} = \frac{2d_{PT}}{v} = \tau_{P_0T_0}(1 + \mu_P + \mu_T) \qquad (14)$$

where d_{PT} is the distance difference of d_1 and d_2; $\tau_{P_0T_0}$ is the time difference at the initial temperature T_0 and initial pressure P_0, which can be derived by Equation 15.

$$\tau_{P_0T_0} = \frac{2d_{P_0T_0}}{v} \qquad (15)$$

where $d_{P_0T_0}$ is the distance difference of d_1 and d_2 at the initial temperature T_0 and initial pressure P_0.

Summarising Equation 11 – 15, φ_{PT} can be derived by Equation 16, and $\varphi_{P_0T_0}$ can be derived by Equation 17.

$$\varphi_{PT} = \omega_0\tau_{PT} = \omega_0\frac{2d_{P_0T_0}}{v}(1 + \mu_P + \mu_T) = \omega_0\frac{2d_{P_0T_0}}{v}(1 + \beta\Delta P + \alpha\Delta T) \qquad (16)$$

$$\varphi_{P_0T_0} = \omega_0\frac{2d_{P_0T_0}}{v} \qquad (17)$$

where $\varphi_{P_0T_0}$ is the phase difference between the response signals reflected by R_1 and R_2 at the initial temperature T_0 and initial pressure P_0.

Therefore, $\Delta\varphi_{PT}$, the subtraction of φ_{PT} and $\varphi_{P_0T_0}$ can be derived by Equation 18.

$$\Delta\varphi_{PT} = \varphi_{PT} - \varphi_{P_0T_0} = \omega_0\frac{2d_{P_0T_0}}{v}(\beta\Delta P + \alpha\Delta T) \qquad (18)$$

Therefore, ΔP can be derived by using ΔP and $\Delta\varphi_{PT}$ (see Equation 19).

$$\Delta P = \frac{v}{2\beta\omega_0 d_{P_0T_0}}\Delta\varphi_{PT} - \frac{\alpha}{\beta}\Delta T \qquad (19)$$

The relations between the phase difference change and the temperature and pressure change are derived, which is shown in Equation (10) and (19). The phase difference change is linear to the temperature change and pressure change.

IV. EXPERIMENT VERIFICATION

Shown in Fig. 3, the signal generator, the signal analyser and the oscilloscope work as the function of the reader for the wireless passive SAW sensor node. The practical experiment set up is shown in Fig. 4. The temperature is controlled by the water bath, which is connected to the outer layer of the glass tube. Water with specific temperature circulates between the water bath container and the outer layer of the glass tube. The castor oil pressure control platform is connected to the strictly sealed inner chamber of the glass pipe. Based on the Boyle's Law, the pressure applied via the platform is equal to the air pressure sensed by the sensor node. The Function/Arbitrary Waveform Generator (Agilent 33220A) generates the pulse signal to mix with the standard 425 MHz sine wave generated by the ESG Vector Signal Generator (Agilent E4438C). The multiplication result of the two signals is transmitted out as the interrogation signal to the sensor node. The 1 GHz Mixed Signal Oscilloscope (Agilent MSO6104A) and the Spectrum Analyser (HP 8563E) receive and process both the interrogation signal and the response signals. Based on the previous studies in [3], the centre frequency of these sensor nodes is 425 MHz, and the best interrogation pulse width is 1 µs. The following experiments are undertaken by the above settings.

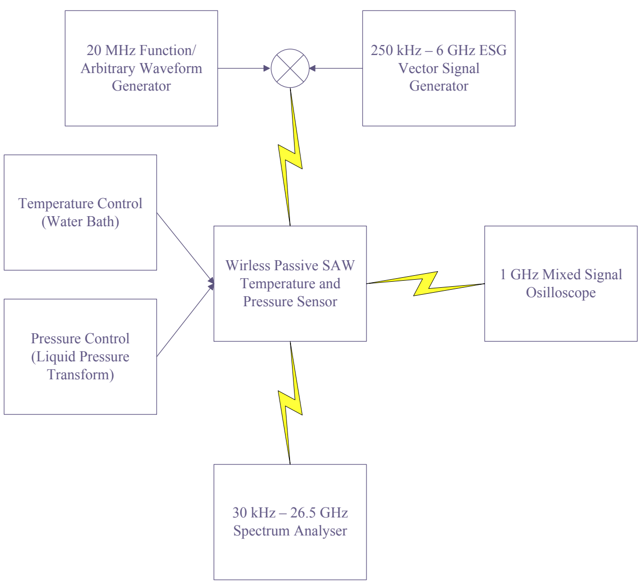

Fig. 3. Wireless interrogation, response and signal analysis with temperature and pressure control.

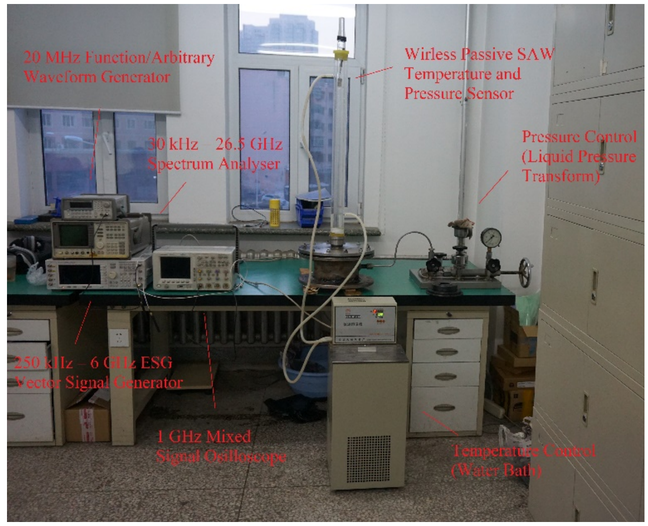

Fig. 4. The picture of the practical experiment set up.

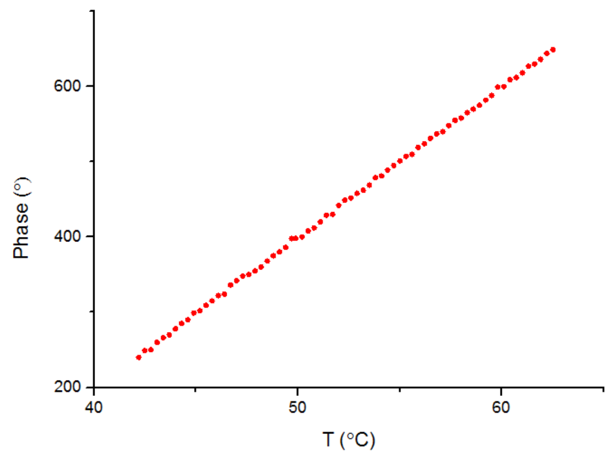

Fig. 5. The relation between the phase delay and temperature when the pressure keeps constant.

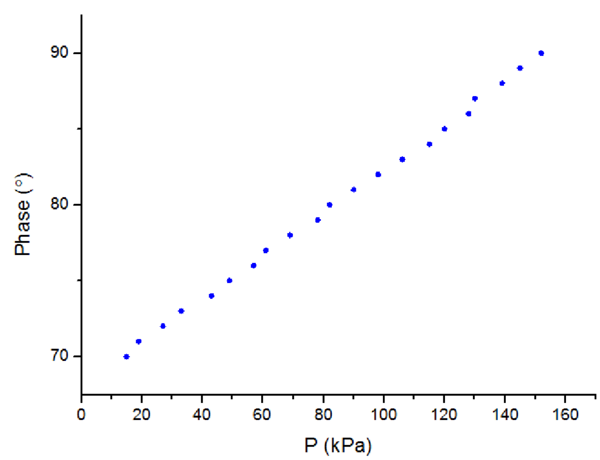

Fig. 6. The relation between the phase delay and pressure when the temperature keeps constant.

The actual temperature and pressure change can be read from the temperature and pressure control platforms, while the experimental values can be obtained through the data of the interrogation and response signals received and processed by the signal analyser and the oscilloscope.

V. CONCLUSION

A wireless passive SAW temperature and pressure delay line sensor was adapted in a designed framework which can control the ambient liquid temperature and pressure and characterised. The results showed that the related phase delay of the response signal depends linearly on the temperature when the pressure keeps constant, and the related phase delay of the response signal depends linearly on the pressure when the temperature keeps constant. The experimental results meet the theoretical relations well.

ACKNOWLEDGMENT

The authors acknowledge the financial support of the European Framework Program (FP7) WatERP (318603) and FP7 Marie Curie Actions-SmartWater (318985) and H2020-ITN-IOT4win (765921) and the support of Dr.Tianli Li from Shenzhen University China

REFERENCES

[1] G. Bruckner, J. Bardong, C. Gruber, and V. Plessky, "A wireless, passive ID tag and temperature sensor for a wide range of operation," Procedia Engineering, vol. 47, pp. 132-135, 2012.

[2] A. Kang, C. Zhang, X. Ji, T. Han, R. Li, and X. Li, "SAW-RFID enabled temperature sensor," Sensors and Actuators: A, Physics, vol. 201, pp. 105-113, 2013.

[3] Z. Tang, W. Wu, and J. Gao, "Water pressure sensing based on wireless passive SAW technology," 13th International Conference on Computing and Control for the Water Industry, CCWI2015, Procedia Engineering, vol.119, pp. 892-900, 2015.

[4] C. Lin, C. Hung, and H. Lin, "A study of wireless torque sensing based on SAW sensors," 2010 International Symposium on Computer, Communication, Control and Automation (3CA), vol. 2, pp. 211-214, 2010.

[5] Y. Wang, Z. Li, L. Qin, M. Chyu, and Q. Wang, "Theoretical and experiemntal studies of a surface acoustic wave flow sensor," IEEE Transactions on Ultrasonics, Ferroelectrics, and Frequency Control, vol. 59, No. 3, pp. 481-490, 2012.

[6] D. C. Malocha, M. Gallagher, B. Fisher, J. Humphries, D. Gallagher and N. Kozlovski, "A Passive Wireless Multi-Sensor SAW Technology Device and System Perspectives," Sensors, vol. 13, pp. 5897–5922, 2013.

[7] T. Li, "Passive SAW temperature and pressure sensor based on tire pressure moniyoring system," Dissertation for the Doctoral Degree in Engineering, Harbin Institute of Technology, 2009.

[8] J. Qi, P. Yang, M. Hanneghan and S. Tang, "Multiple density maps information fusion for effectively assessing intensity pattern of lifelogging physical activity," Neurocomputing, vol. 220, pp.199-209, 2017.

[9] J. Qi, P. Yang, D. Fan and Z. Deng, "A survey of physical activity monitoring and assessment using internet of things technology," In Computer and Information Technology; Ubiquitous Computing and Communications; Dependable, Autonomic and Secure Computing; Pervasive Intelligence and Computing (CIT/IUCC/DASC/PICOM), 2015 IEEE International Conference on, pp. 2353-2358, 2015.

[10] J. Qi, P. Yang, M. Hanneghan, D. Fan, Z. Deng and F. Dong, "Ellipse fitting model for improving the effectiveness of life-logging physical activity measures in an Internet of Things environment," IET Networks, vol. 5, No. 5, pp.107-113, 2016.

[11] J. Qi, P. Yang, G. Min, O. Amft, F. Dong and L. Xu, "Advanced internet of things for personalised healthcare systems: A survey," Pervasive and Mobile Computing, vol. 41, pp.132-149, 2017.

[12] P. Yang, M. Hanneghan, J. Qi, Z. Deng, F. Dong and D. Fan, "Improving the validity of lifelogging physical activity measures in an internet of things environment," In Computer and Information Technology; Ubiquitous Computing and Communications; Dependable, Autonomic and Secure Computing; Pervasive Intelligence and Computing (CIT/IUCC/DASC/PICOM), 2015 IEEE International Conference on, pp. 2309-2314, 2015.

[13] J. Qi, P. Yang, M. Hanneghan, K. Latham and S. Tang, "Uncertainty Investigation for Personalised Lifelogging Physical Activity Intensity Pattern Assessment with Mobile Devices," In Internet of Things (iThings) and IEEE Green Computing and Communications (GreenCom) and IEEE Cyber, Physical and Social Computing (CPSCom) and IEEE Smart Data (SmartData), 2017 IEEE International Conference on, pp. 871-876, 2017.

[14] P. Yang and W. Wu, "Efficient Particle Filter Localization Algorithm in Dense Passive RFID Tag Environment," IEEE Transactions on Industrial Electronics, vol. 61(10), pp. 5641 – 5651, 2014.

[15] P. Yang, W. Wu, M. Moniri and C. Chibelushi, "Efficient Object Localization Using Sparsely Distributed Passive RFID Tags," IEEE Transactions on Industrial Electronics, vol. 60(12), pp. 5914 - 5924, 2013.

[16] Z. Tang, W. Wu, J. Gao and P. Yang, "Feasibility Study on Wireless Passive SAW Sensor in IoT Enabled Water Distribution System," In Internet of Things (iThings) and IEEE Green Computing and Communications (GreenCom) and IEEE Cyber, Physical and Social Computing (CPSCom) and IEEE Smart Data (SmartData), 2017 IEEE International Conference on, pp. 830-834, 2017.